Mass, velocity, angular and charge-state distributions from the fusion of ^{32}S and ^{112}Sn

C. Bolton and W. A. Schier*
Department of Physics, University of Lowell, Lowell, Massachusetts 01854

N. Tsoupas, H. Enge, M. Salomaa, and A. Sperduto
Laboratory for Nuclear Science, Massachusetts Institute of Technology, Cambridge, Massachusetts 02139

A. Graue
Department of Physics, University of Bergen, Bergen, Norway
(Received 2 November 1977)

Evaporation residues from the fusion of ^{32}S and ^{112}Sn at $E_{^{32}S} = 160$ MeV were studied using an energy-mass spectrometer. The velocity selector of the energy-mass spectrometer was first utilized to measure summed fusion products as a function of velocity setting and reaction angle. In-flight mass separation of the fusion products with the energy-mass spectrometer identified masses 141, 140, and 139 from the evaporation of three to five nucleons from the ^{144}Dy compound nucleus. Absolute cross-section measurements are compared to theoretical predictions of the statistical evaporation model. Velocity, angular and charge state distributions of evaporation residues are also compared to calculated values.

[NUCLEAR REACTIONS $^{32}S+^{112}Sn$ fusion, $E=160$ MeV, $\sigma(v,\theta)$. Compared mass, velocity and angular distributions of evaporation residues to statistical particle evaporation theory. Compared charge-state distribution of fusion products to semiempirical predictions.]

I. INTRODUCTION

As part of our experimental program to produce proton-rich nuclei of ever greater mass by means of heavy-ion reactions, a study of the fusion of ^{32}S and ^{112}Sn at an incident energy of 160 MeV was undertaken and is discussed here. Earlier studies within our group of the mass distributions of evaporation residues following the complete fusion of heavy ions included the $^{32}S+^{58}Ni$ and $^{32}S+^{70}Ge$ reactions.[1] All three reactions utilized targets of the most neutron-deficient stable isotope for each element so that new or not well-known isotopes are created lying far off the β-stability line on the proton-rich side. Ultimately it may be possible to detect super-heavy nuclei via fusion reactions. If so, the compound system will by necessity be proton rich. Measurements on systems of ever greater mass could therefore yield some important guidelines for the attack on the super heavies.

In this work both the total evaporation residue cross section and the relative cross section for the individual A chains were measured for the $^{112}Sn(^{32}S,x\mathcal{Y})^{144-x}X$ reactions employing the MIT-BNL energy-mass spectrometer (EMS). The experimental results are compared with calculations from the computer code ALICE.[2]

II. EXPERIMENTAL PROCEDURE

The energy-mass spectrometer [Fig. 1(a)] is comprised of a Wien velocity filter, which separates the beam from the low velocity fusion products, and a modified split-pole magnetic spectrograph.[3] The magnetic spectrograph disperses the fusion products in the horizontal direction on the focal plane according to their momentum/charge ratio. The velocity filter displaces the

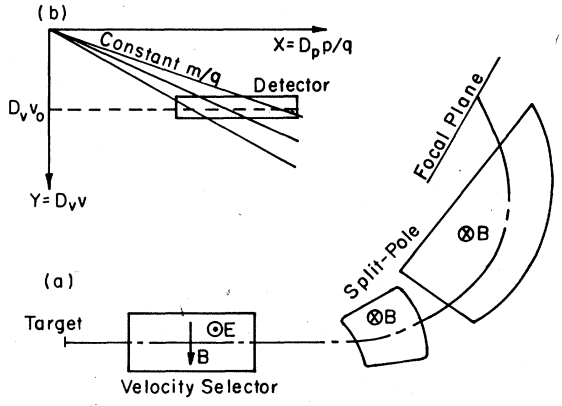

FIG. 1. (a) Schematic diagram of the energy-mass spectrograph. (b) Representation of dispersions in the detector plane.

masses vertically according to their velocity. The instrument is double-focusing (stigmatic). Hence particles with a given mass/charge ratio produce a sharp slanted line on the focal plane [see Fig. 1(b)]. The calculated mass resolution for the instrument varies from $m/\Delta m = 440$ to $m/\Delta m = 360$ over the range covered, assuming a 1-mm target spot. A resolution of $m/\Delta m = 430$ has been demonstrated. A detailed description of the design and operation of the EMS has been given by Enge and Horn.[4]

A 160-MeV ^{32}S beam from the MP tandem Van de Graaff accelerator at BNL bombarded a 140-μg/cm^2 ^{112}Sn target made by evaporation of SnO_2 (73% enriched in ^{112}Sn) onto a 12-μg/cm^2 carbon backing stabilized with a flash of gold. Normalization to an absolute cross-section scale was achieved by monitor detectors at 41.4° in the scattering chamber. By taking tin/gold elastic ratios from well below the Coulomb barrier to 160 MeV, it was ascertained that the tin elastics were essentially Rutherford. The impurity isotopes of tin in the target are expected to contribute about the same fusion/elastic ratio as that for ^{112}Sn and should therefore not substantially affect the total cross-section measurement. Since several impurity isotopes were present, each in small amounts, they are expected to form a general background in the mass spectrum.

Due primarily to nucleon evaporation, the mass residues following fusion were dispersed both in velocity (about $v_{\text{c.m.}}$) and in angle (about 0°). The spectrometer was, therefore, utilized here in two ways to study the fusion reaction. By employing only the velocity filter portion of the EMS and a 600-mm^2 surface barrier detector, the velocity and angular dependencies of the summed evaporation residues were first measured. Then the full EMS was employed to obtain the mass distribution at a representative velocity and angle. Ideally the mass distribution should be measured as a function of both velocity and angle but constraints on beam time precluded such a lengthy procedure.

III. THEORETICAL CONSIDERATIONS

Theoretical comparisons to experimental measurements were made in three areas: the mass distribution and total fusion cross section of evaporation residues, the dispersion in velocity and angle of the fusion products from nucleon evaporation, and the charge-state distribution of the fusion products.

Theoretical predictions of the mass distributions and total cross sections were calculated for the $^{112}\text{Sn}(^{32}\text{S}, x\mathfrak{N})^{144-x}X$ reaction at 160 MeV with the computer code ALICE.[2] Calculations were also made with the code CASCADE[5]; however, because of its excessive use of computer time, there was no opportunity to adjust the evaporation parameters. With the built-in parameters (default mode) the program predicted much too large cross sections for α evaporation.

The parabolic-potential parameters used for the incident channel in the code ALICE are

$$V = 67 \text{ MeV},$$

$$R = 1.17\,(A_1^{1/3} + A_2^{1/3})\,\text{fm},$$

$$a = 0.57 \text{ fm}.$$

For the proton and neutron exit channels a volume-absorption type Woods-Saxon potential, utilizing the global parameters of Perey[6] (protons) and of Wilmore and Hodgson[7] (neutrons) was used. α particles were parametrized with the potential of Huizenga and Igo.[8] Nuclear binding energies were calculated by means of the Myers-Swiatecki[9] mass formula.

The measured velocity profiles and angular distribution for the evaporation residues deal with a sum over all the heavy nuclides that were formed in the fusion-evaporation process. In order to make a rigorous comparison between experiment and theory, one would have to calculate velocity and angular distributions as a weighted sum over a large number of evaporation channels. The appropriate weighting factors, of course, are not known theoretically, nor can they be determined from our present measurements since only the mass distribution is measured. Therefore a more modest objective is proposed here, namely, to demonstrate that a simple multiple nucleon emission calculation agrees satisfactorily with the measured velocity and angular distribution of the evaporation residues. Due to the low-neutron evaporation energy, compared to that of a proton, neutron boiloff changes the recoil distributions imperceptibly only. Therefore, only the effect of proton evaporation was calculated in this work (e.g., a three-proton, two-neutron cascade was approximated by three-proton emission). Calculations made with the in-house program BETH[10] are based on a 25% two-proton, 51% three-proton, and 24% four-proton emission and assume isotropic angular distributions of the protons. The percentages are estimated from ALICE predictions modified to agree with the measured mass distribution (see Discussion section). The BETH code parametrizes the velocity distribution of the neutrons and protons (in the c.m. system) as

$$\sigma_n(v) \propto E e^{-0.9E},$$

$$\sigma_p(v) \propto \begin{cases} \sqrt{E}(E-E_0)^{1/2} e^{-0.24(E-E_0)}, & E > E_0, \\ 0, & E < E_0, \end{cases}$$

where $E_0 = (0.96ZA^{-1/3} - 5.2)$ MeV. The center-of-mass velocity distribution for α particles is somewhat more detailed because the barrier cutoff region is also approximated. The distribution peaks at an energy, E_m, and

$$\sigma_\alpha(v) \propto \begin{cases} \sqrt{E}(E-E_1)^{1/2} e^{-0.21(E-E_1)}, & E > E_m, \\ -a(E-E_m)^2 + b, & E_m - 4 < E < E_m, \\ 0, & E < E_m - 4, \end{cases}$$

where $E_m = (0.206Z + 2.53)$ MeV, $E_1 = 15.3$ MeV. All energies are in MeV and the constants a and b are determined by boundary matching conditions. These velocity distributions for neutrons, protons, and α particles are generated from measured evaporation spectra[11-13].

The velocity distributions of the evaporation residues were measured with the velocity selector alone. Unlike the complete EMS this device does not produce a sharp velocity spectrum, but convolutes velocity with direction of emission from the target. Thus

$$\int_{-\infty}^{+\infty} f(v)\Omega(v - v_0)dv = F(v_0),$$

where $f(v)$ is the true velocity distribution, $\Omega(v - v_0)$ is the velocity dependent solid angle, and $F(v_0)$ is the measured velocity distribution as a function of velocity selector setting $v_0 = E/B$. The BETH code performs this convolution and also converts center-of-mass distributions to the laboratory system, a process which is equivalent to taking the Jacobian:

$$\frac{d^2\sigma_{\text{c.m.}}}{d\Omega_{\text{c.m.}}\,dv_{\text{c.m.}}} \Big/ \frac{d^2\sigma_l}{d\Omega_l\,dv_l} = |J| = \left| \frac{\partial(\cos\theta_l)}{\partial(\cos\theta_{\text{c.m.}})} \frac{\partial(v_l)}{\partial(v_{\text{c.m.}})} - \frac{\partial(\cos\theta_l)}{\partial(v_{\text{c.m.}})} \frac{\partial(v_l)}{\partial(\cos\theta_{\text{c.m.}})} \right| = \left(\frac{v_{\text{c.m.}}}{v_l}\right)^2.$$

The charge-state distribution of the 34-MeV evaporation residues is compared both as to the predicted average charge and the width of the distribution. The average charge state is calculated using the semiempirical formulas of Betz *et al.*,[14]

$$\bar{q}/z = 1 - C \exp -\left(\frac{v}{v_0 z^\gamma}\right),$$

where $C = 1.03$, $\gamma = 0.517$, and $v_0 = 2.188 \times 10^8$ cm/s, and of Nikolaev and Dmitriev[15],

$$\bar{q}/z = [1 + (z^{-\alpha} v/v')^{-1/k}]^{-k},$$

where $\alpha = 0.45$, $k = 0.6$, and $v' = 3.6 \times 10^8$ cm/s. The width of the charge distribution expressed as a standard deviation is calculated from the semiempirical relation[16]

$$d = d_1 z^w,$$

with $d_1 = 0.27$ and $w = 0.5$ according to Betz.[17] A somewhat more recent width estimate[14] for solid strippers is also tested:

$$d = d_2 \bar{q}[1 - (\bar{q}/z)^{1/k}]^{1/2},$$

where $d_2 = 0.5$ and $k = 0.6$.

IV. DATA ANALYSIS

Summed evaporation residues from the fusion of ^{32}S and ^{112}Sn were initially studied with the velocity filter portion of the EMS. The energy spectrum in Fig. 2 displays excellent discrimination between evaporation residues and background events arising mainly from sulfur ions in the low-energy tail of the beam which meet the filter's velocity conditions. Measured velocity profiles of these fusion products are given in Fig. 3.

Angular distributions of fusion products integrated at each angle over velocity are given in Fig. 4. The shape of the distribution is approximated by a Gaussian with $\theta_{\text{HWHM}} = 4°$ corresponding to a standard deviation $w = 3.4°$ or 0.059 rad. When this distribution is integrated over solid angle one obtains

$$\sigma_T = 2\pi w^2 Y_m \quad \text{(valid for } \sigma \ll 1 \text{ rad)},$$

where Y_m is the peak cross section at 0°. The total fusion cross section for these evaporation residues obtained in this manner is 511 ± 70 mb. The cross-section uncertainty estimate arises mainly from the target composition and the angular distribution shape which is only approximately Gaussian.

Figure 5 displays a mass spectrum of evaporation residues measured at 3° and at the center of the experimental velocity profile using the full EMS with 10-μm K-2 Ilford nuclear emulsions as detectors. Since the spectrometer accepts a ±1° angular increment, the 3° data actually represent a 2° to 4° integral at the center velocity of the

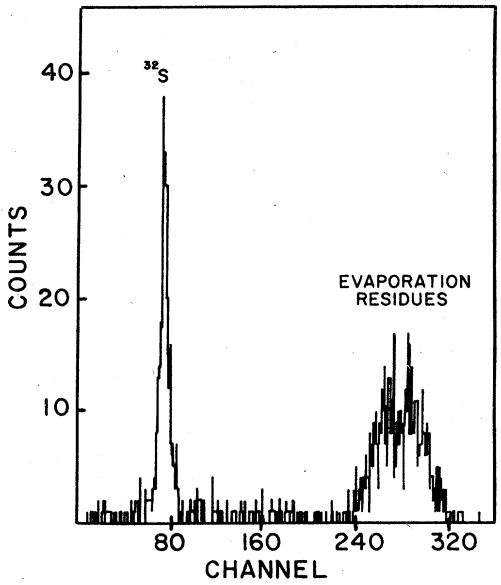

FIG. 2. A sample energy spectrum of summed evaporation residues from the fusion of ^{32}S and ^{112}Sn at $E_{^{32}S}$ = 160 MeV taken with a surface barrier detector in the auxilliary chamber and utilizing only the velocity selector portion of the energy-mass spectrograph. The sulfur line arises from ^{32}S ions in the tail of the beam meeting the velocity conditions of the Wien filter.

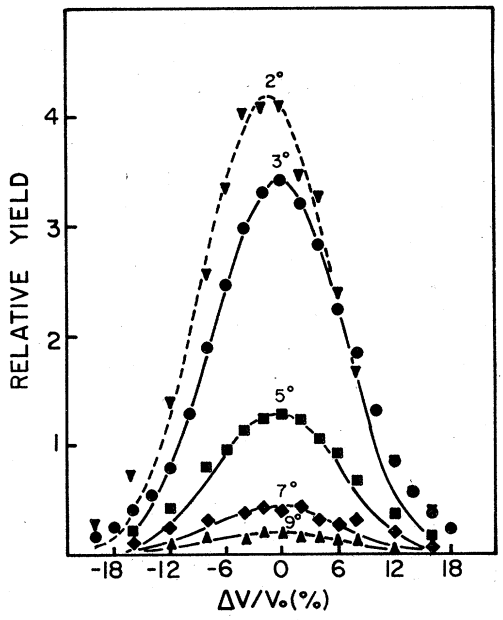

FIG. 3. Velocity profiles of the summed fusion products measured as a function of velocity setting of the Wien filter and of the reaction angle. The curves are peak normalized laboratory velocity distributions calculated with BETH assuming 25% two-proton, 51% three-proton and 24% four-proton evaporation. The shift in the 2° data is not understood and probably not a real effect. The dashed curve indicates the curve is shifted accordingly.

measured profile. The three dominant masses at this angle and velocity are 139, 140, and 141 with the mass signature repeating itself for charge states 15 through 21. This 3° measurement gives mass ratios that are considered representative of total mass ratios since the laboratory velocity profiles and angular distributions calculated by BETH for each mass line are quite similar. A sulfur peak is also observed in the spectrum. It arises from elastic scattering of that part of the low-energy tail of the beam that has the correct velocity to pass through the velocity selector. It provides a calibration line for the measured mass and charge distributions. The resolution increases with distance along the focal plane up to $D = 100$ cm. In this spectrum the resolution is less than premium due mainly to beam spot instability. Measured mass ratios obtained from this spectrum are listed in Table I.

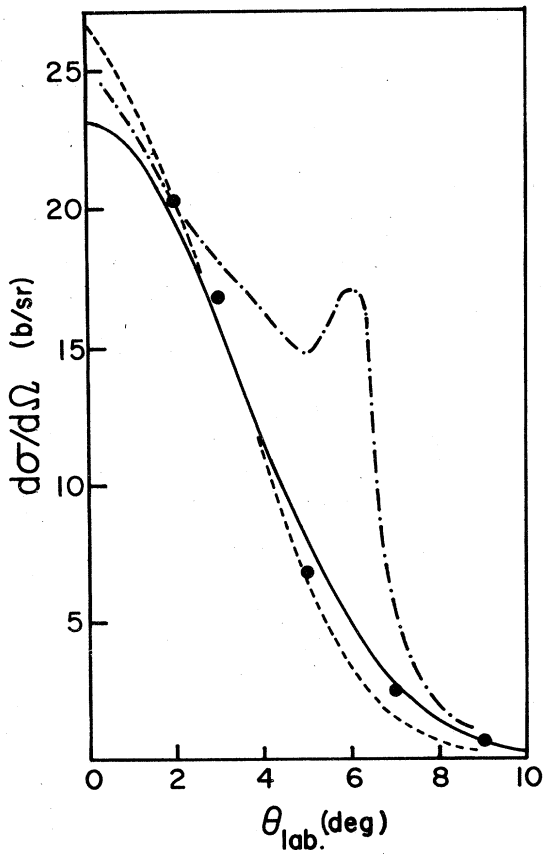

Fig. 4. The angular distribution of evaporation residues integrated at each angle over velocity. The solid curve is a Gaussian distribution fit. The dashed curve is the laboratory angular distribution calculated with BETH assuming 25%(2p)-51%(3p)-24%(4p). The dash-dot curve assumes that masses 139 and 140 (but not mass 141) are produced completely through α emission so that the total mix is 15%(2p)-13%(3p)-42%(1α)-30%(1α,1p) distribution.

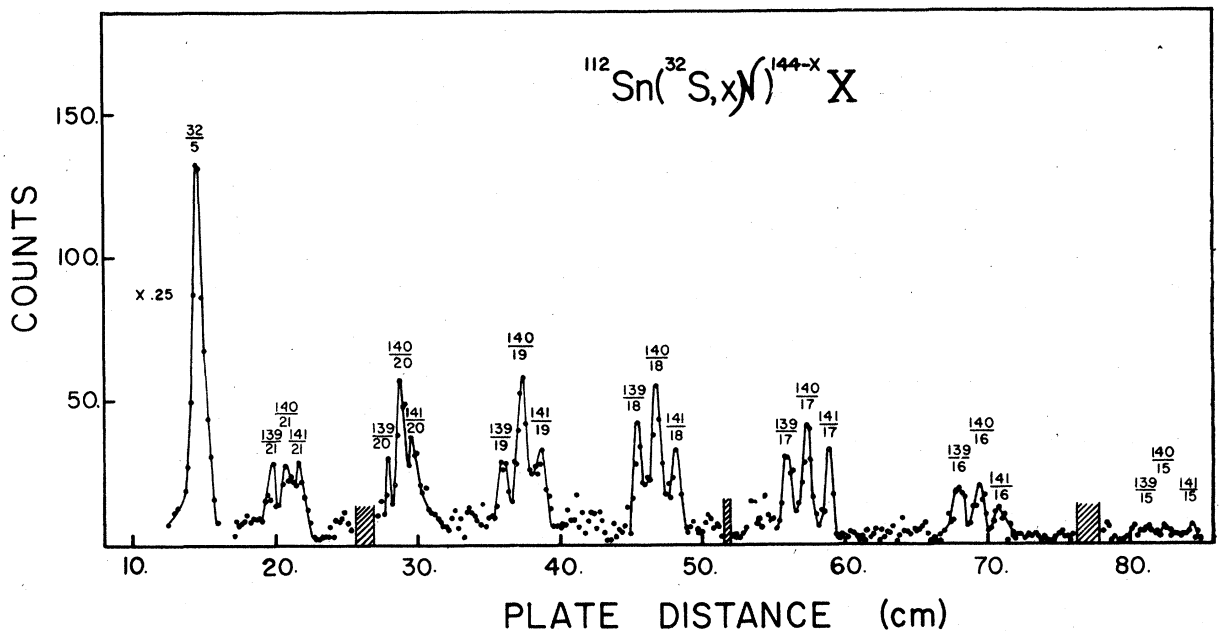

Fig. 5. A mass spectrum taken with the full energy-mass spectrograph at the peak of the measured 3° velocity profile. Masses 141, 140 and, 139 from $^{112}Sn(^{32}S,xN)^{144-x}X$ reaction are identified with the mass signature repeating itself for charge states 15 through 21. The sulfur peak serves as a useful calibration point.

The charge-state distribution for the 34-MeV fusion products is plotted in Fig. 6. A Gaussian was fitted to the data having a mean charge state of $\bar{q} = 18.7$ and a half width at half maximum $\Delta q_{HWHM} = 2.7$ charge states, corresponding to a standard deviation of 2.3 charge states.

V. DISCUSSION AND CONCLUSION

The measured residual mass ratios are compared in Table I to the predictions of the computer code ALICE. The experimental percentages of masses ≤138 are given with large uncertainties because the other tin isotopes present in the target do contribute a general background of overlapping mass/charge-state lines which could account for much of the yield in the region of the $A = 132$–138 mass lines.

The ALICE calculation qualitatively agrees with experimental values. A non-negligible mass 141 cross section is predicted and the other dominant mass lines, 140 and 139, are nearly in quantitative agreement. The total evaporation residue cross section calculated with ALICE is 613 mb, compared with the experimental value of 511 ± 70 mb. ALICE also predicts a 33 mb fission cross section.

To calculate the velocity and angular distributions with BETH, masses 139, 140, and 141 were assumed to be the sole contributors, and the ALICE results were adjusted to give the measured ratios for these three masses while preserving the rela-

TABLE I. Calculated cross sections in millibarns for evaporation residues following the fusion of ^{32}S and ^{112}Sn at 160 MeV. Prediction from the statistical evaporation code ALICE are given and compared with experimental cross sections (percentages).

A	Z							$\Sigma\sigma_{th}$		σ_{exp}
	65	64	63	62	61	60	59	(mb)	(%)	(%)
141	4.0	28.4	23.8					56.2	9.2	26
140	1.5	42.3	128.0	45.1				216.9	35.4	38
139		4.4	47.5	56.8	4.5			113.2	18.5	27
138		1.1	18.4	17.6	0.9			38.0	6.2	2 ± 2
137		0.2	17.1	66.9	17.3			101.5	16.6	4 ± 4
136			0.8	21.7	27.2	1.3		51.0	8.3	1.5 ± 1.5
135				2.2	5.0	0.1		7.3	1.2	1.5 ± 1.5
134				1.1	13.5	5.6		20.2	3.3	
133					1.9	6.1	0.3	8.3	1.3	
132						0.3		0.3	· · ·	

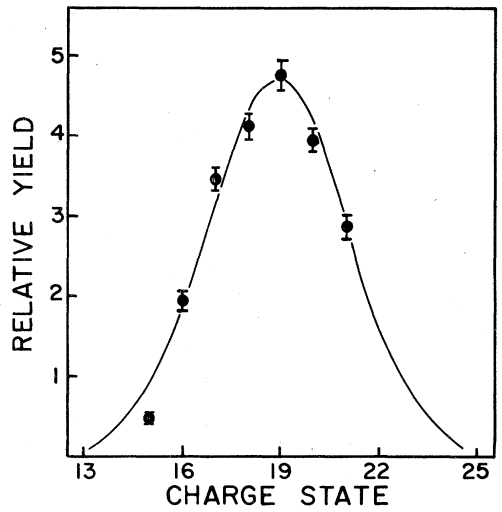

Fig. 6. The plotted data are the measured distribution of charge states from the summed 139, 140, and 141 mass lines. A Gaussian fit to the data is obtained with $\bar{q}=18.7$ and $\Delta q_{\mathrm{HWHM}}=2.7$.

tive isotopic cross sections in the production of a particular mass. This leads to the 25%($2p$)-51%($3p$)-24%($4p$) mix used in the calculation ($1p$ and $5p$ contributions were assumed negligible). The calculated center-of-mass velocity distributions of the fusion products in Fig. 7 converted to the laboratory system were convoluted with the solid-angle function (Fig. 8) calculated with the program RAYTRACE.[18] The resulting velocity distribution curves are shown in Figs. 3 and 9. Effects of target thickness on the velocity and angular distributions were also considered and found to be very small. The width of the true velocity

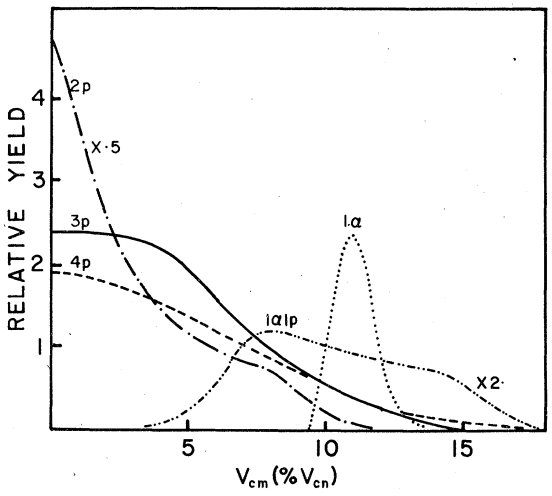

Fig. 7. Center-of-mass velocity distributions of evaporation residues calculated with BETH from the evaporation of two, three, and four protons, one α particle, and one α plus one proton.

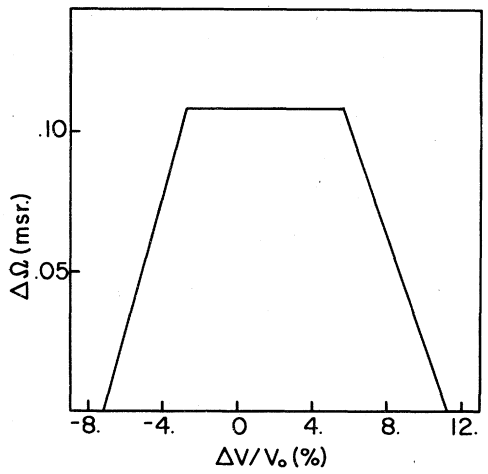

Fig. 8. The solid angle of the velocity filter as a function of velocity calculated with the program RAYTRACE.

profile increases by less than 0.1% in $\Delta v/v$ when energy loss and straggling effects are added in quadrature. Multiple scattering added in quadrature increased the calculated width at half height of the angular distribution by less than 0.1°.

Had the mass 139 and 140 A chains been formed by α emission, the angular distribution and measured velocity profiles would have markedly different shapes as indicated in Figs. 4 and 9. The true velocity profile (Fig. 9) in this case would have two sharp peaks at $\Delta v/v$ values of ±10% although the convolution with the solid-angle function produces a "measured" profile that is not as distinctive. In contrast, the angular distribution (Fig. 4) would retain its sensitivity to α boiloff with a sharp secondary peak appearing in the cross section at 6°. Our measured angular distribution and velocity profiles gave no indication that α emission was significant in the formation of the mass 139 and 140 A chains.

Excitation functions generated by ALICE and presented in Fig. 10 suggest the energy dependence of the formation probability for the most important A chains. The predicted yield of mass 139 could artificially be increased by a small shift to a higher energy bringing the calculation nearer to the measured value, although the mass 141 yield would fall still lower.

The measured distribution of charge states ($\bar{q}=18.7$ $\Delta q_{\mathrm{HWHM}}=2.7$) is compared to the semiempirical formulas by setting $A=140$, $Z=63$, and $E=33.6$ MeV (a target thickness correction has been applied here). The relations of Betz *et al.*[14,17] give $\bar{q}=17.9$ and $\Delta q_{\mathrm{HWHM}}=2.33$ while the equations of Nikolaev and Dmitriev[15] predict $\bar{q}=17.1$ and $\Delta q_{\mathrm{HWHM}}=2.52$. In Betz's mean charge-state relationship, the constants C and γ are based on data

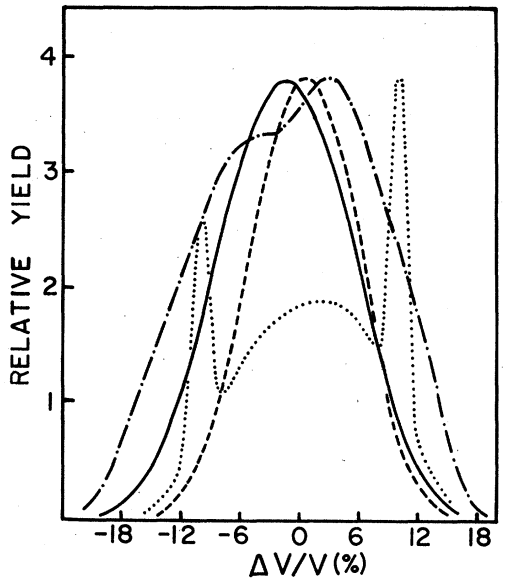

Fig. 9. Velocity profiles at 3° in the laboratory system generated with the program BETH. The dashed curve assumes a 25%($2p$)-51%-($3p$)-24%($4p$) distribution. This curve, when convoluted with the solid-angle function, broadens into the solid curve. The dotted curve arises from the 15%($2p$)-13%($3p$)-42(1α)-30%(1α, $1p$) mix. When convoluted with the solid-angle function, the dashed-dot curve is formed. For comparison purposes, the curves have been normalized to the same peak height.

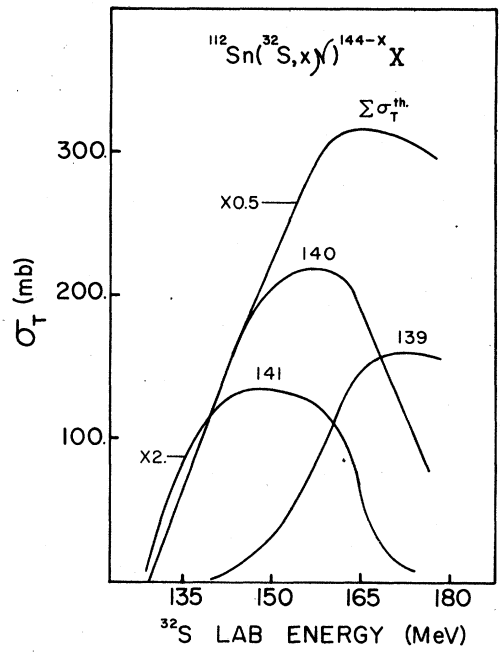

FIG. 10. Excitation functions calculated with ALICE for the three dominant masses, 139, 140, and 141, and for the total cross section.

from a Formvar stripper. A dependence of the mean charge state on the composition of the stripper foil has been observed.[17] At these energies, a shift downward of approximately two charge states would be expected when replacing a carbon stripper by one of gold. In our case, the ^{112}Sn target is the stripper foil, and this would place the predicted value of the mean charge state near $\bar{q}$ = 16 in poor agreement with the measurement $\bar{q}$ = 18.7. It should be noted that the charge-state distributions of evaporation residues immediately following the reaction most likely are quite different from those of similar ions with the same speed but in charge equilibrium inside the foil. In particular it should be noted that the ^{32}S ions that initiate the reaction are either completely stripped or very nearly so.

The measurements of mass and velocity distribution of evaporation residues discussed here are necessary first steps in utilizing the EMS to separate individual A chains for further study. We plan to measure lifetimes and decay schemes of the positron emitters in each A chain by x-ray and γ-ray spectroscopy, employing a tape transport system to carry the evaporation residues from either the auxilliary chamber of the velocity selector or the focal plane of the EMS to the detectors. The tape speed is adjusted so as to optimize on each isotope's lifetime. The tape transport system is operational and preliminary results have been reported.[19]

In summary, we have found that this medium-mass fusion reaction has a large evaporation residue cross section. The proton-rich ^{144}Dy compound nucleus has a preference to deexcite by proton boiloff with α emission being quite negligible.

ACKNOWLEDGMENTS

This work was supported in part by the U. S. Energy Research and Development Administration under Contract No. EY-76-C-02-3069. Two of the authors, C. Bolton and W. Schier, wish to express their deep appreciation for the hospitality extended to them by members of the Laboratory for Nuclear Science at MIT and tandem lab at BNL. We particularly thank Professor E. Cosman for making the formal arrangements. Discussions with Dr. G. Couchell concerning the center-of-mass to lab conversion of cross sections are gratefully acknowledged. Dr. H. Wegner and T. Yeager graciously provided us with the CASCADE calculation.

*Associated with the Laboratory for Nuclear Science, MIT, while on sabbatical leave from the University of Lowell.

[1]D. Horn, H. A. Enge, A. Sperduto, and A. Graue Phys. Rev. 17, 118 (1978).
[2]M. Blann and F. Plasil, U. S. Atomic Energy Commission Report No. COO-3494-10, 1973 (unpublished).
[3]J. E. Spencer and H. A. Enge, Nucl. Instrum. Methods 49, 181 (1967).
[4]H. A. Enge and D. Horn, Nucl. Instrum. Methods 145 (1977) 271.
[5]F. Pulhofer (unpublished).
[6]F. G. Perey, Phys. Rev. 131, 745 (1963).
[7]D. Wilmore and P. E. Hodgson, Nucl. Phys. 55, 673 (1964).
[8]J. R. Huizenga and G. Igo, Nucl. Phys. 29, 462 (1961).
[9]W. D. Myers and W. J. Swiatecki, Nucl. Phys. 81, 1 (1966).
[10]C. Bolton, University of Lowell (unpublished).
[11]W. J. Knox, A. R. Quinton, and C. E. Anderson, Phys. Rev. 120, 2120 (1960).
[12]I. Dostrovsky, Z. Fraenkel, and L. Winsberg, Phys. Rev. 118, 781 (1960).
[13]D. M. Skyrme, Nucl. Phys. 35, 183 (1962).
[14]H. D. Betz, G. Hortig, E. Leischner, Ch. Schmelzer, B. Stadler, and J. Weilhrauch, Phys. Lett. 22, 643 (1966).
[15]V. S. Nikolaev and I. S. Dmitriev, Phys. Lett. 28A, 277 (1968).
[16]I. S. Dmitriev and V. S. Nikolaev, Sov. Phys. JETP 20, 409 (1965).
[17]H. D. Betz, Rev. Mod. Phys. 44, 465 (1972).
[18]H. A. Enge and S. B. Kowalski, in Proceedings of the International Conference on Magnet Technology, Hamburg, 1970 (unpublished), p. 366.
[19]P. E. Haustein, W. Schier, M. Salomaa, and H. A. Enge, Bull. Am. Phys. Soc. 22, 8 (1977).